A Study on the Distribution and Uniformity of Symmetric Extended TEM Cells

Chunjiang Song [1], Yuntao Jin [2], and Fei Dai [2,*]

[1] Department of Engineering Physics
Tsinghua University, Beijing, 100084, China

[2] School of Electronic and Information Engineering
Beihang University, Beijing, 100191, China
*daphige@buaa.edu.cn

Abstract ─ TEM Cells can generate computable standard fields, which are often used in electromagnetic measurement systems. Their electromagnetic field uncertainty has a great influence on the evaluation of system measurement results. In this paper, a method and index for rigorous evaluation of the uniformity of electromagnetic field distribution in the test area are presented. The relationship between different measurement accuracies and the size limits of the test object is analyzed by HFSS. According to this relationship, the limit condition of the sample size is established when the E field measurement accuracy is 1dB. Among them, the height requirements are consistent with the traditional experience requirements, and the width requirements are more stringent. On this basis, the electric field distribution law of the symmetric extended TEM chamber is studied and analyzed. It shows that the field uniformity of the symmetric extended TEM room is basically unchanged when the test space is multiplied.

Index Terms ─ Electric field, field uniformity, TEM Cells, uncertainty.

I. INTRODUCTION

TEM Cells consist of a rectangular outer conductor and a core between the top and bottom layers. As the name suggests, the standard TEM Cell is essentially a two-conductor transmission line that operates in TEM mode. In the case of additional excitation and matching loads, a computable standard field [1] can be constructed. In IEEE 1309-2013 [2], it is recommended to use TEM cells below 200 MHz as a common generation device for probe calibration systems.

To ensure the validity of the measurement results, the TEM Cells are used in the electromagnetic measurement system. The main problems are the accurate calculation of the standard field and the uncertainty evaluation of the system measurement results. For the standard field calculation, it is mainly related to the measurement of the net power P_{net}, the characteristic impedance real part Z_0 and the TEM cell half height d of the TEM Cells [3]. The uncertainty assessment of the system measurement results is mainly determined by the uncertainty of the standard field generated by the TEM Cells. When Crawford [1] proposed the design of TEM Cells in 1974, it made a preliminary assessment of its calibration uncertainty and proposed a method to correct the field disturbance of the electric field [4]. Lu's [5] research suggests that field distortion is not easy to predict, so it is necessary to limit the size of the test object. However, the effect of position on the field in the original TEM Cells is not given.

Most of the current research focuses on the uncertainty of the standard field generated by standard TEM cells, but there are few studies on the uncertainty of TEM cells after expanding the test space. Wilson and Ma proposed asymmetric TEM cells [6]. K. Malathi studied the extended characteristic impedance of asymmetric TEM cells [7]. Virginie proposed a three-dimensional TEM cell [11]. Dai and Song et al. proposed TEM cells with dual and quadruple symmetric extensions [9,10]. Based on the standard TEM Cell field uniformity analysis, the field distribution and uniformity of symmetrically extended TEM cells are further studied in this paper.

II. FIELD UNIFORMITY ANALYSIS OF STANDARD TEM CELLS

According to IEEE STD 1309-2013 [2], the characteristic impedance of TEM Cells is calculated by the following formula:

$$Z_0 = \frac{94.2}{\frac{w}{b}+\frac{2}{\pi}ln[1+coth(\frac{\pi g}{2b})]}, \quad (1)$$

where the b, g, w is given in the Fig. 1.

Submitted On: August 27, 2018
Accepted On: October 12, 2018

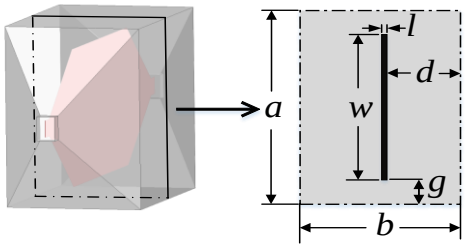

Fig. 1. Cross section of a basic TEM Cell.

In general, the characteristic impedance is designed to be 50 ohms to match the impedance of the measurement system. The field strength in the TEM Cells is calculated according to the formula (2) where P_{net} is the input net power of the TEM cells:

$$E = \frac{\sqrt{P_{net} Z_0}}{d}. \quad (2)$$

For Model I proposed by Hill [11], $Z_0 = 51.7\Omega$ can be obtained from formula (1); substituting $P_{net} = 1W$, d=1.5m into formula (2) can get E=4.8V/m. In fact, the electric field distribution in the TEM Cells is not completely uniform, and there will be obvious distortion on both sides of the core board. To this end, it is generally required that the width of EUT does not exceed a/2, and the height does not exceed d/3 (or b/6); for more accurate tests, the height does not even exceed d/5 [2]. This empirical requirement does not fully explain the degree of field uniformity. Therefore, in this paper, the mean (E_{mean}), standard deviation (E_{SD}), coefficient of variation (CV_E), dynamic range (DR_E), etc. of the E field in the test area are used to indicate the field uniformity.

The mean of the E field can be used to describe the level of the built-in E field of the TEM Cells for a given input net power. To compare the performance difference between different TEM cells, this paper uses the mean of the field strength, when the input field power is 1W, E_{mean}^{1W} as a parameter.

Both the standard deviation and the coefficient of variation can describe the dispersion of the electric field values in the test area. The smaller they are, the more concentrated the electric field value distribution is in the mean:

$$CV_E = \frac{E_{SD}}{E_{mean}}. \quad (3)$$

Formula (3) shows that CV_E is the result of normalization of E_{SD} relative to E_{mean}, which is more general.

E_{mean}^{1W} and CV_E illustrate the statistical properties of the built-in E field of TEM Cells, and the dynamic range shows the maximum differences in the distribution of E field values:

$$DR_E = 20 \times \log\left(\frac{E_{max}}{E_{min}}\right). \quad (4)$$

Model I was simulated by HFSS in Driven Modal to study the field uniformity of the test area. Based on the requirements of traditional experience, the original test area is divided into three areas according to the height. The height of these areas is about d/3, and the test area at each height is further divided into three according to the width. There are 9 test areas for a/6, d/3, and a/2, as shown in Fig. 2 and Table 1. These test areas are on the cross section of the middle section of the TEM Cells along the direction of the signal propagation, and the cross section is parallel to the XZ plane. On each test area, the height (Z axis) is divided into 15-line segments, and 16 test points are evenly arranged for each line segment, for a total of 240 test points. From the E field simulation results of 240 points, the mean (E_{mean}^{1W}), coefficient of variation (CV_E) and dynamic range (DR_E) of each test area are calculated, as shown in the Figs. 3-5.

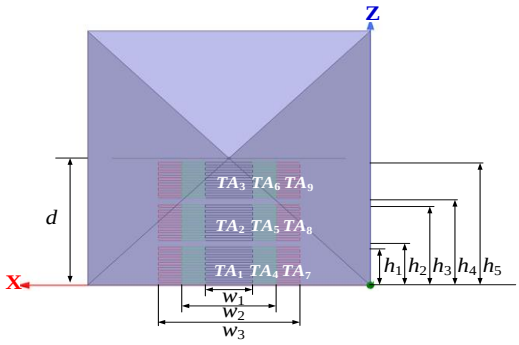

Fig. 2. Test areas divided in Model I.

Table 1: 9 test areas in the Model I

Test Area	Width (m)	Lower Limit (m)	Upper Limit (m)	Height (m)
No. 1	$w_1 = 0.5$	0.03	$h_1 = 0.45$	0.42
No. 2	$w_1 = 0.5$	$h_2 = 0.53$	$h_3 = 0.95$	0.42
No. 3	$w_1 = 0.5$	$h_4 = 1.03$	$h_5 = 1.45$	0.42
No. 4	$w_2 = 1$	0.03	$h_1 = 0.45$	0.42
No. 5	$w_2 = 1$	$h_2 = 0.53$	$h_3 = 0.95$	0.42
No. 6	$w_2 = 1$	$h_4 = 1.03$	$h_5 = 1.45$	0.42
No. 7	$w_3 = 1.5$	0.03	$h_1 = 0.45$	0.42
No. 8	$w_3 = 1.5$	$h_2 = 0.53$	$h_3 = 0.95$	0.42
No. 9	$w_3 = 1.5$	$h_4 = 1.03$	$h_5 = 1.45$	0.42

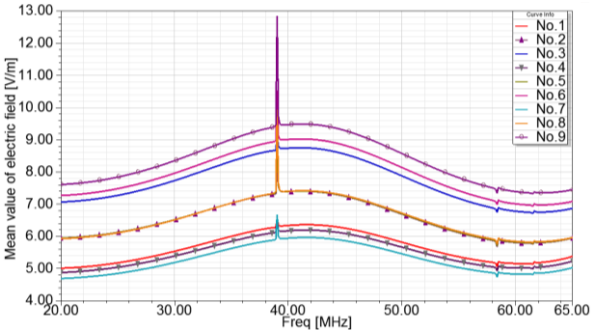

Fig. 3. Mean value of E field.

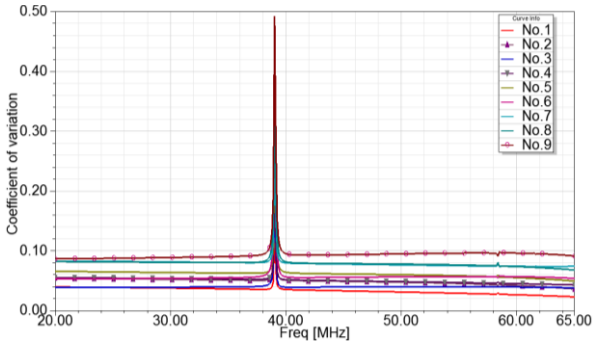

Fig. 4. Coefficient of variation of E field.

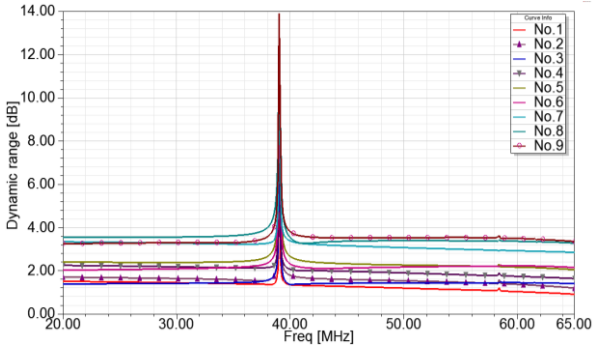

Fig. 5. Dynamic range of E field.

Figures 3-5 show three extreme points with frequencies of 39.01MHz, 58.36MHz, and 61.62MHz, which are consistent with the resonant frequencies calculated in the Eigen Mode of Table 1, corresponding to the TE011, TE012, and TE101 modes, respectively. In the TEM Cells of the Model I, since the propagation mode is the TEM mode, the frequency band lower than 39.01 MHz can be used. In the TEM mode, the average E field strength in the bottom region of the TEM cells is about 5 V/m, which is equivalent to the calculation result of the formula (2). What's more, analysis of Figs. 3-5 can lead to the following conclusions:

1) The magnitude of the field strength is related to the position of the test area. The closer the E field is to the bottom, the smaller the E field is. The closer it is to the septum which is no more than 2 times the bottom field strength, the bigger the E field is.
2) The change in the coefficient of variation indicates that the smaller the width of the test area, the more uniform the electric field distribution. Although the electric field distribution in the bottom test area is relatively more uniform, the effect of the position is not significant. The coefficient of variation for all regions is less than 0.1, indicating that the electric field distribution in TEM Cells is generally uniform.
3) The dynamic range presents a similar law to the coefficient of variation. When the test area height is d/3, the maximum difference of the electric field value is less than 2dB when the width is only a/6, which indicates that for the precision test such as E field probe calibration, the conventional upper limit of a/2 is too loose.

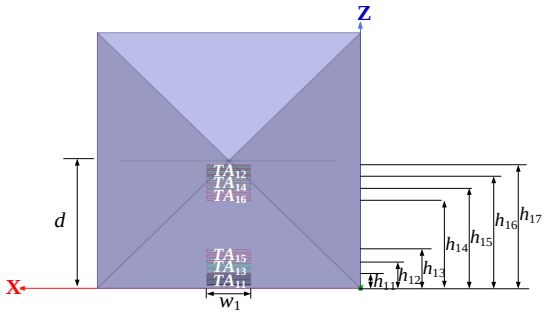

Fig. 6. Test areas divided in Model I.

Table 2: 9 test areas in the Model I

Test Area	Width (m)	Lower Limit (m)	Upper Limit (m)	Height (m)
No. 11	$w_1 = 0.5$	0.03	$h_{11} = 0.17$	0.14
No. 12	$w_1 = 0.5$	$h_{16} = 1.31$	$h_{17} = 1.45$	0.14
No. 13	$w_1 = 0.5$	0.03	$h_{12} = 0.31$	0.28
No. 14	$w_1 = 0.5$	$h_{15} = 1.17$	$h_{17} = 1.45$	0.28
No. 15	$w_1 = 0.5$	0.03	$h_{13} = 0.45$	0.42
No. 16	$w_1 = 0.5$	$h_{14} = 1.03$	$h_{17} = 1.45$	0.42

Further, the influence of the height and position of the test area on the uniformity of the field was analyzed. According to the above conclusion (1), two regions with a height of d/3 and a width of a/6 close to the core plate and the bottom are selected, and the two regions are divided into three test regions by the height of the region. The height of each test area is *d*/9, 2*d*/9, d/3, as shown in Fig. 6 and Table 2. On each test area, the height (Z axis) is divided into 15-line segments, and 16 test points are evenly arranged for each line segment, for a total of 240 test points. From the E field simulation results of 240 points, the mean (E_{mean}^{1W}), coefficient of variation (CV_E) and dynamic range (DR_E) of each test area are calculated, as shown in Figs. 7-9.

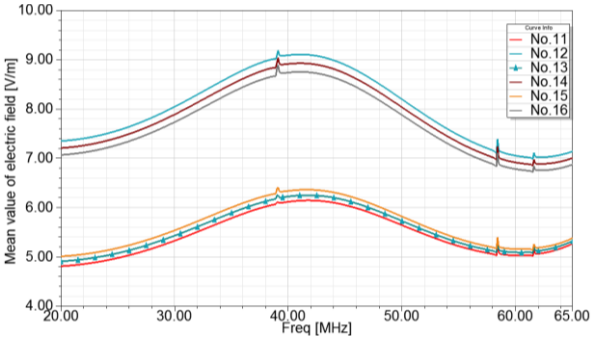

Fig. 7. Mean value of E field.

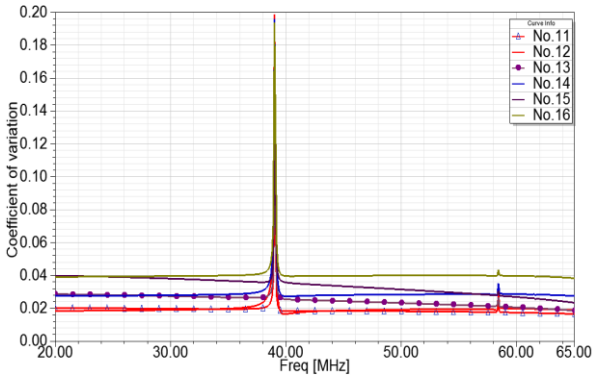

Fig. 8. Coefficient of variation of E field.

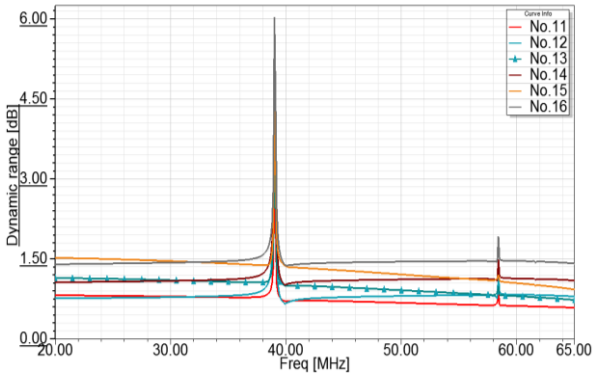

Fig. 9. Dynamic range of E field.

Figure 7 and Fig. 3 show the same law: the magnitude of the field strength is related to the position of the test area. The closer to the bottom, the E field is smaller. The closer to the septum which is no more than the bottom field strength, the E field is bigger. Figure 8 shows that the smaller the height of the test area, the smaller the coefficient of variation, and the coefficient of variation is not significantly affected by the position. Although the height of the test area has an influence on the coefficient of variation, the coefficient of variation in the six cases of Fig. 8 are all less than 0.05. Further, in combination with Fig. 4, it can be found that the coefficient of variation is approximated by the law of the width and height of the test area. The dynamic range of Fig. 9 shows a similarity to the coefficient of variation. When the height of the test area does not exceed d/3, the maximum difference of the E field value is 1.5 dB. When the height of the test area does not exceed 2*d*/9, the maximum difference of the E field value is 1 dB.

From this we can conclude that when the amplitude measurement accuracy within the TEM Cells is required to be better than 1 dB, the width of the test area cannot exceed a/6 and the height cannot exceed *d*/5. This result is stricter than the provisions of the existing standards.

III. ELECTRIC FIELD DISTRIBUTION LAW IN DUAL CELLS

In Fig. 10, the bottom walls/plates of two identical TEM Cells are bonded together first and removed then. When the cells of the symmetric TEM cells are differentially excited and the same power P_{net} is input, the voltage difference between the internal spacers becomes twice that of the ordinary TEM cells, but the distance between the spacers becomes 2d, so the internal field strength can still be calculated by formula (2).

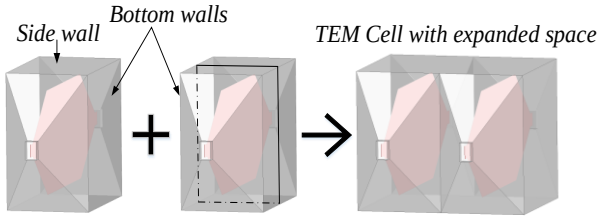

Fig. 10. A symmetric Extended TEM Cells.

Taking symmetric binary TEM cells as an example, let the input signal of one of the ports be:

$$V_1 = V^{j\varphi}. \tag{5}$$

Then the ideal signal for the other port (differential port) input should be:

$$V_2 = V^{j(\varphi+\pi)}. \tag{6}$$

If the phase of V_2 is not ideal, it can be expressed as:

$$V_2 = V^{j(\varphi+\theta+\pi)}. \tag{7}$$

If the magnitude of V_2 is not ideal, it can be expressed as:

$$V_2 = V^{j(\varphi+\theta+\pi)}. \tag{8}$$

The paper using HFSS analyzes the effect of the phase θ within $\pm 5°$ and the amplitude error does not exceed $\pm 10\%$ on the electric field in the TEM Cells. The simulation model is shown in Fig. 11, where $w_1 = 0.5\text{m}$, $h_{21} = 0.28\text{m}$ and test areas TA_{21} and TA_{22} are TA_{13} and TA_{14} doubled in height, respectively.

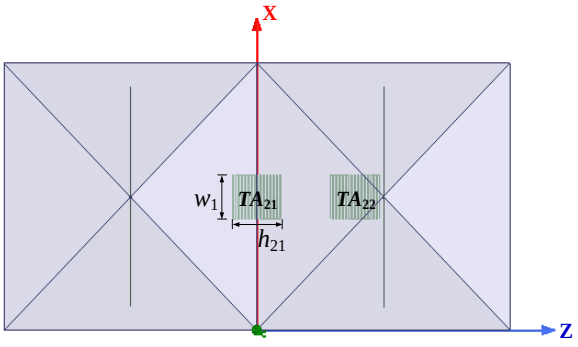

Fig. 11. Symmetric extended TEM Cells.

The simulation frequency is set at 25MHz, and the internal electric field of the TEM Cells is the TEM mode. The reference port in the differential input port has an input power of 1W and a phase of 0°. According to the range of amplitude and phase accuracy of the general signal source, the input power range of the other input port is 0.9~1.1W, and the phase is 175~185°. The simulation results are shown in Figs. 12-17.

Figures 12-17 show that after the TEM cells are symmetrically expanded into dual chambers, the bottom can be multiplied by the test area, and the ability to generate electric fields and field uniformity is consistent with a single TEM Cell. When the phase error of the input differential signal does not exceed ±5° and the amplitude error does not exceed ±10%, the disturbance to the electric field can be neglected.

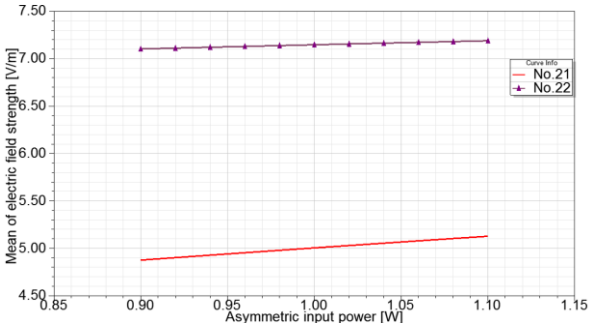

Fig. 12. E field strength vs. Asymmetric input power.

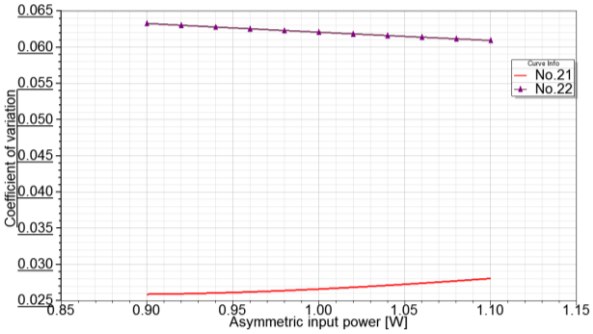

Fig. 13. Coefficient of variation vs. Asymmetric input power.

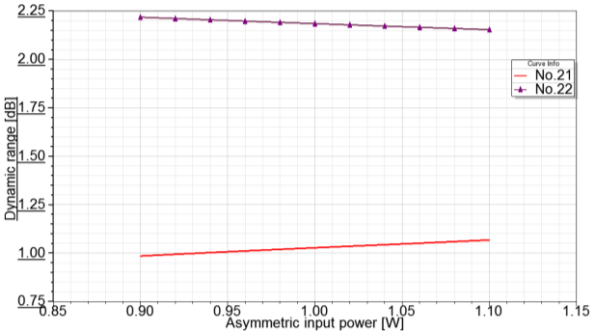

Fig. 14. Dynamic range vs. Asymmetric input power.

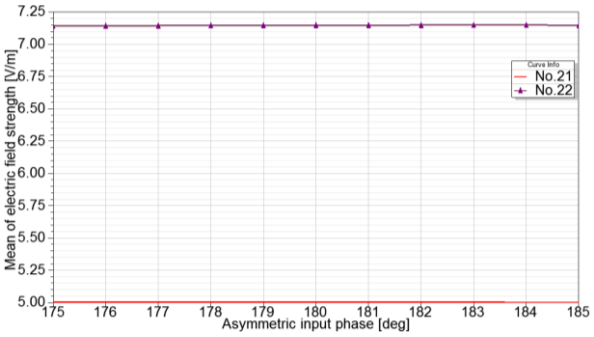

Fig. 15. E field strength vs. Asymmetric input phase.

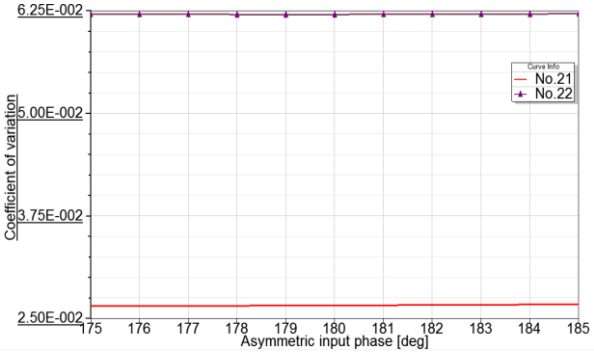

Fig. 16. Coefficient of variation vs. Asymmetric input phase.

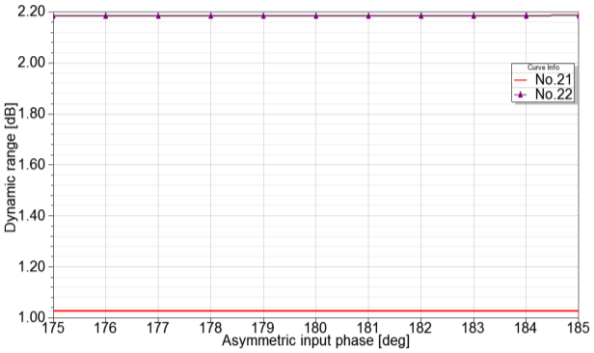

Fig. 17. Dynamic range vs. Asymmetric input phase.

IV. CONCLUSION

Based on the field-average value, this paper further proposes the method of describing the field uniformity in standard TEM cells by parameters such as standard deviation (E_{SD}), coefficient of variation (CV_E), dynamic range (DR_E) etc. Based on these indicators, the relationship between different measurement accuracy requirements and the size of the test object was determined, and a method for rigorously assessing the uniformity of electromagnetic field distribution in the test area was given. In the traditional experience requirements, when the electric field measurement accuracy requirement is 1dB, the width of the test

object cannot exceed a/6, and the height cannot exceed d/5.

In this paper, the electric field distribution of symmetrically extended TEM cells is further studied. Studies have shown that after the TEM cells are multiplied into double chambers with test areas, their ability to generate electric fields and field uniformity are consistent with standard TEM cells. Based on the accuracy range of the existing signal source, it is found that when the input differential signal phase error does not exceed $\pm 5°$ and the amplitude error does not exceed $\pm 10\%$, the influence of the input signal error on the electric field generated in the TEM cells can be ignored.

Based on the research content of this paper, the law of electric field distribution and uniformity after loading the test object in symmetric extended TEM cells will be studied, and the factors affecting the uncertainty of symmetric extended TEM cells will be further analyzed.

ACKNOWLEDGMENT

This work is supported in part by the National Natural Science Foundation of China. (Grant No. 61571027, 61427803), and supported by the 2011 Collaborative Innovation Center.

REFERENCES

[1] M. L. Crawford, "Generation of standard EM fields using TEM transmission cells," *IEEE Transactions on Electromagnetic Compatibility*, vol. EMC-16, no. 3, pp. 189-195, Nov. 1974.

[2] IEEE. STD 1309-2013, IEEE Standard for Calibration of Electromagnetic Field Sensors and Probes, Excluding Antennas, From 9 kHz to 40 GHz, 2013.

[3] M. T. Ma, M. Kanda, M. L. Crawford, and E. B. Larsen, "A review of electromagnetic compatibility/ interference measurement methodologies," *Proceedings of the IEEE*, vol. 73, no. 3, pp. 388-411, Mar. 1985.

[4] M. L. Crawford and J. L. Workman, "Using a TEM Cell for EMC Measurement of Electronic Equipment," *U. S. National Bureau of Standards Technical Note 1013*, Apr. 1979.

[5] X. Lu, "Characteristic impedance variation of the TEM cell caused by the introduction of the equipment under test," *IEICE/IEEE International Symposium on Electromagnetic Compatibility*, Tokyo, Japan, pp. 596-599, May 1999.

[6] P. Wilson and M. Ma, "Simple approximate expressions for higher order mode cutoff and resonant frequencies in TEM cells," *IEEE Transactions on Electromagnetic Compatibility*, vol. 28, no. 3, pp. 125-130, Aug. 1986

[7] K. Malathi and D. Annapurna, "Numerical analysis of impedance of asymmetric TEM cell filled with inhomogeneous, isotropic dielectric," *Applied Computational Electromagnetics Society Journal*, vol. 19, pp. 39-45, 2004.

[8] D. Virginie, "Optimization of three-dimensional TEM cell for electromagnetic compatibility testing," *20th Annual Review of Progress in Applied Computational Electromagnetics*, 2004.

[9] F. Dai, M. Wang, and D. L. Su, "A design of new twin TEM cells," *IEEE 2005 International Symposium on Microwave, Antenna, Propagation and EMC Technologies for Wireless Communications Proceedings*, vol. 1, pp. 10-13, 2005.

[10] C. J. Song and X. Y. Feng, "A new design and implementation of expanding testing space of a transverse electromagnetic cell," *The 9th International Conference on Microwave and Millimeter Wave Technology*, vol. 2, pp. 967-969, 2016.

[11] D. A. Hill, "Bandwidth limitation of TEM cells due to resonances," *Journal of Microwave Power*, vol. 18, no. 2, pp. 181-195, 1983.

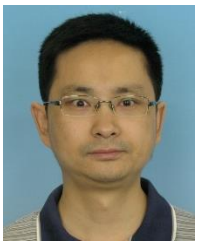

Chunjiang Song joined the Department of Engineering Physics in Tsinghua University, Beijing, China, in 2012 and he is currently working toward the Ph.D. degree. His research interests include the microwave technology, electronic measurement technology, and EMC technology.

Yuntao Jin receive the B.Eng. degree in Electronic Engineering from Soochow University, Jiangsu, China, in 2017, and he is currently working towards the M.S. degree in the School of Electronic and Information Engineering at Beihang University. His research interests include the microwave technology and EMC technology.

Fei Dai receive the Ph.D. degree in Circuits and Systems from Beihang University, Beijing, China, in 2007. He joined the Electromagnetic Compatibility Laboratory at Beihang University, Beijing, in 2007, where he is currently an Associate Professor. His research interests include the EMC technology, microwave technology, and antennas technology.